Astron. Astrophys. 360, 417–430 (2000)

ASTRONOMY AND ASTROPHYSICS

Comptonization of the cosmic microwave background by relativistic plasma

T.A. Enßlin and C.R. Kaiser

Max-Planck-Institut für Astrophysik, Karl-Schwarzschild-Str. 1, D-85740 Garching, Germany

Received 26 January 2000 / Accepted 20 June 2000

Abstract. We investigate the spectral distortion of the cosmic microwave background (CMB) caused by relativistic plasma. Within the Thomson regime, an exact analytic expression for the photon scattering kernel of a momentum power-law electron distribution is given, which is valid from the non- to the ultra-relativistic regime. The decrement in the photon spectrum saturates for electron momenta above $3\,m_{\rm e}\,c$ to that of an optically thick absorber with the optical depth of the relativistic electrons given by the Thomson limit. Thus, the ultra-relativistic Sunyaev-Zeldovich (SZ) decrement measures the electron number and not the energy content. On the other hand, the relativistic SZ increment at higher frequencies depends strongly on the spectral shape of the electrons, allowing for investigation of relativistic electron populations with future instruments.

We calculate the expected Comptonization due to the energy release of radio galaxies, which we estimate to be $\approx 3\cdot 10^{66}\,{\rm erg\,Gpc^{-3}}$. We investigate Comptonization from (a) the part of the released energy which is thermalized and (b) the relativistic, remnant radio plasma, which may form a second, relativistic phase in the intergalactic medium, nearly unobservable for present day instruments (presence of so called 'radio ghosts'). We find a thermal Comptonization parameter due to (a) of $y\approx 10^{-6}$ and (b) an optical depth of relativistic electrons in old radio plasma of $\tau_{\rm rel}\leq 10^{-7}$. If a substantial fraction of the volume of clusters of galaxies is filled with such old radio plasma the SZ effect based determination of the Hubble constant is biased to lower values, if this is not accounted for. Finally, it is shown that a supra-thermal population of electrons in the Coma cluster would produce a signature in the Wien-tail of the CMB, which is marginally detectable with a multifrequency measurement by the Planck satellite. Such an electron population is expected to exist, since its bremsstrahlung would explain Coma's recently reported high energy X-ray excess.

Key words: cosmology: cosmic microwave background – radiation mechanisms: non-thermal – scattering – galaxies: intergalactic medium – galaxies: active – galaxies: clusters: individual: Coma

Send offprint requests to: T.A.E.
Correspondence to: T.A.E., (ensslin@mpa-garching.mpg.de) and C.R.K., (kaiser@mpa-garching.mpg.de)

1. Introduction

The Sunyaev-Zeldovich (SZ) effect has proven to be an important tool for cosmology and the study of clusters of galaxies. It measures the total thermal energy content of the electron population along a line of sight and does not depend on spectral features of the underlying electron distributions, as long as they are non-relativistic. For a review see Sunyaev & Zeldovich (1980).

Deviations in the spectral shape of the SZ effect occur for higher electron temperatures or energies, increasing from the mildly, through the trans- to the ultra-relativistic regime. Approximation for relativistic corrections to the thermal SZ effect are given in the literature. For reviews see Rephaeli (1995a), Fargion & Salis (1998), Molnar & Birkinshaw (1999), Birkinshaw (1999), and Sazonov & Sunyaev (2000).

The thermal SZ effect (thSZ) is therefore a calorimeter for heat releasing processes in the universe, such as the gravitational compression of matter during structure formation, and the energy output of galaxies. A very violent form of energy release of galaxies are the outflows of relativistic plasma from active galactic nuclei. This plasma fills large volumes, the radio lobes, and thereby forms very low density cavities filled with relativistic particles and magnetic fields (for evidence for these cavities see: Böhringer et al 1995; Carilli & Harris 1996; Carilli & Barthel 1996; Clarke et al. 1997; McNamara et al. 2000). The replaced inter-galactic medium (IGM) is heated by this process (e.g. Kaiser & Alexander 1999). It is one goal of this work to estimate the amount of this energy and its imprint on the CMB (see also Enßlin et al. 1998b; Yamada et al. 1999).

Also the radio plasma is able to Comptonize the CMB. A search for the SZ effect in radio lobes was carried out by McKinnon et al. (1991). After being released from the radio galaxy, the relativistic electrons with the highest energies cool rapidly due to synchrotron and inverse Compton (IC) losses, letting the radio lobes fade away after the AGN stops its activity. Patches of such remnant, undetectable radio plasma were named 'radio ghosts' (Enßlin 1999). However, the less energetic electrons may remain relativistic in such an environment for cosmological times. Compton scattering off these electrons removes photons from the CMB Planck spectrum and scatters them to much higher energies, leading to an SZ effect with a characteristic spectral signature.

Since radio ghosts are a still speculative ingredient of the IGM, we discuss different strategies to reveal their presence. We further discuss their possible influence on the SZ effect in clusters of galaxies.

The paper is organized as follows. In Sect. 2 we discuss the theory of transrelativistic inverse Compton (IC) scattering. In Sect. 4 we examine the possible role radio ghosts can have, and estimate their contribution to the CMB-Comptonization. In Sect. 5 we discuss the possible influence remnant radio plasma in the ICM can have on the determination of the Hubble parameter via the SZ effect (Sect. 5.1). Further SZ measurements of cluster of galaxies are proposed as a tool to test for non-thermal electrons in the intra-cluster medium (Sect. 5.2). Conclusions can be found in Sect. 6.

We assume an Einstein de Sitter (EdS) cosmology and $H_\mathrm{o} = 50\,h_{50}\ \mathrm{km\,s^{-1}\,Mpc^{-1}}$. All IC calculations are done in the optically thin limit.

2. Comptonization of the CMB

2.1. Phenomenology of SZ-effects

We distinguish here three processes which change the spectral shape of the CMB by inverse Compton scattering:

- the thermal Sunyaev-Zel'dovich effect (thSZ),
- the kinetic Sunyaev-Zel'dovich effect (kSZ),
- up-scattering of photons by relativistic electrons (rSZ).

The latter happens whenever a CMB photon gets scattered off a relativistic electron. An electron with gamma factor γ increases the frequency ν of a scattered photon (ν') on average by a factor $\nu'/\nu = \frac{4}{3}\gamma^2 - \frac{1}{3}$. The photon is therefore scattered to much higher energies and is effectively removed from the spectral range of the CMB. We consider a photon to be removed from the CMB, if its energy is increased by about one order of magnitude or greater, requiring $\gamma > 3$. Relativistic electrons with lower γ-factors still produce a substantial energy gain of the photon, which also depopulates the Rayleigh-Jeans side of the CMB, but these electrons are less effective scatterers compared to electrons of higher energies. An accurate way to treat this case is given in Sect. 3.1.

Using the usual Kompaneets approximation and neglecting for the moment those relativistic electrons with $\gamma < 3$, the spectral distortion produced by the three processes under considerations are (see e.g. Rephaeli 1995b)

$$\delta i(x) = g(x)\, y_\mathrm{gas} - h(x)\, \bar{\beta}_\mathrm{gas}\tau_\mathrm{gas} - i(x)\, \tau_\mathrm{rel}\,, \tag{1}$$

where the CMB-blackbody spectrum is

$$I_\nu = i_0\, i(x) = i_0\, \frac{x^3}{e^x - 1}\,, \tag{2}$$

with $x = h\nu/kT$ and $i_0 = 2\,(kT_\mathrm{cmb})^3/(hc)^2$. For comparison: the peak of the spectrum is at $x = 2.82$, and the up-coming Planck satellite will measure the CMB signal at $x = 1.8$, 2.5, 3.8, 6.2, 9.6, and 15 (Bersanelli et al. 1996; Puget 1998; see also Table 2). The thSZ-distortions, which have a spectral shape given by

$$g(x) = \frac{x^4\, e^x}{(e^x-1)^2}\left(x\,\frac{e^x+1}{e^x-1} - 4\right)\,, \tag{3}$$

depend in their strength on the Comptonization parameter

$$y_\mathrm{gas} = \frac{\sigma_\mathrm{T}}{m_\mathrm{e}\,c^2}\int dl\, n_\mathrm{e,gas}\, kT_\mathrm{e}\,. \tag{4}$$

The line-of-sight integral extends from the last scattering surface of the cosmic background radiation at $z = 1100$ to the observer at $z = 0$. The kSZ-distortions have the spectral shape

$$h(x) = \frac{x^4\, e^x}{(e^x-1)^2} \tag{5}$$

and depend on $\bar{\beta}_\mathrm{gas}$, the average line-of-sight streaming velocity of the thermal gas ($v_\mathrm{gas} = \beta_\mathrm{gas}\, c$, $\beta_\mathrm{gas} > 0$ if gas is approaching the observer), and the Thomson optical depth

$$\bar{\beta}_\mathrm{gas}\,\tau_\mathrm{gas} = \sigma_\mathrm{T}\int dl\, n_\mathrm{e,gas}\,\beta_\mathrm{gas}\,. \tag{6}$$

Finally, the optical depth of relativistic electrons

$$\tau_\mathrm{rel} = \sigma_\mathrm{T}\int dl\, n_\mathrm{e,rel} \tag{7}$$

determines the fraction of the number of photons, which are effectively removed from the CMB.

3. Introduction

3.1. Transrelativistic Thomson scattering

We derive here the exact formulae for the photon redistribution function of the transrelativistic SZ effect in the Thomson regime, which can be applied to get the relativistically correct thSZ, but also the rSZ for any arbitrary isotropic electron distribution. Such a formula has already been given in the literature (Rephaeli 1995a), but not in the compact form provided here (see Eq. (21)). We further give the analytically exact photon redistribution function for a power-law electron distribution.

The change in intensity due to IC-scattering of a blackbody photon distribution at an isotropic distribution of electrons in the optical thin limit is given by

$$\delta i(x) = (j(x) - i(x))\,\tau\,, \tag{8}$$

where τ is the Thomson optical depth

$$\tau = \sigma_T\int dl\, n_\mathrm{e}\,. \tag{9}$$

$i(x)\,\tau$ is the flux scattered to other frequencies, and $j(x)\,\tau$ is the flux scattered from other frequencies to $x = h\,\nu/(kT)$. In Eq. (1) we assumed that $j(x) \ll i(x)$ in the region of interest ($x < 10$) for ultra-relativistic electrons. In the following we drop this approximation.

Eq. (8) can be re-written to include a y-like parameter

$$\delta i(x) = \tilde{g}(x)\,\tilde{y}\,, \tag{10}$$

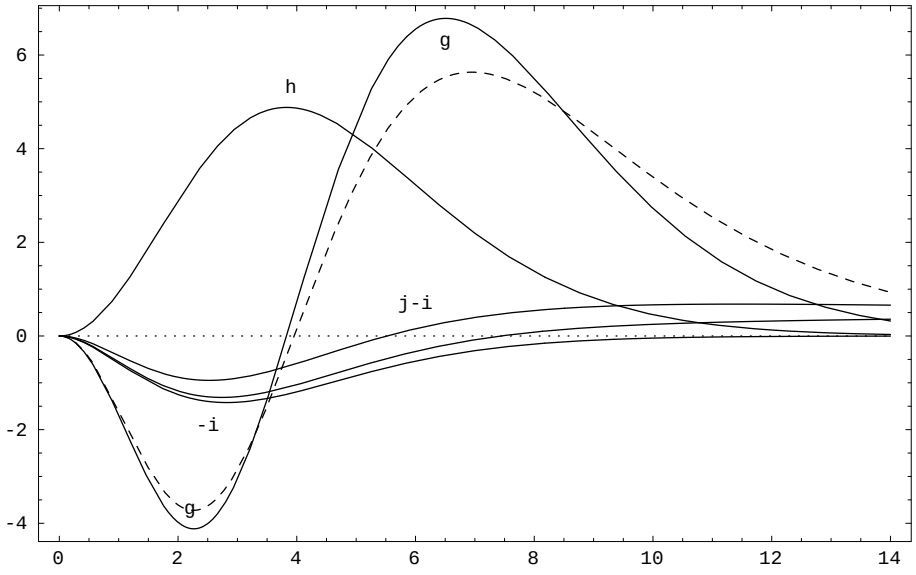

Fig. 1. The functions $g(x)$, $h(x)$, $-i(x)$, and above the latter $j_{\rm cr}(x;\alpha,p_1,p_2)-i(x)$ for $p_1 = 1$, 3 (from top to bottom), $p_2 = 1000$, and $\alpha = 2$. The dashed curve is the relativistic correct, numerically estimated $\tilde{g}(x)$ for a thermal plasma with $kT_{\rm e} = 15$ keV.

where

$$\tilde{y} \;=\; \frac{\sigma_T}{m_{\rm e}\,c^2}\int dl\, n_{\rm e}\, k\tilde{T}_{\rm e} \tag{11}$$

$$k\tilde{T}_{\rm e} \;=\; \frac{P_{\rm e}}{n_{\rm e}} \tag{12}$$

$$\tilde{g}(x) \;=\; (j(x)-i(x))\;\frac{m_{\rm e}\,c^2}{\langle k\tilde{T}_{\rm e}\rangle} \tag{13}$$

$$\langle k\tilde{T}_{\rm e}\rangle \;=\; \frac{\int dl\, n_{\rm e}\, k\tilde{T}_{\rm e}}{\int dl\, n_{\rm e}} \tag{14}$$

with $P_{\rm e}$ the electron pressure (see Eq. (A.6)). The definition of the pseudo-temperature $k\tilde{T}_{\rm e}$ is equal to the thermodynamic temperature in the case of a thermal electron distribution (Eq. (25)).

If one introduces the photon redistribution function $P(t)\,dt$, which gives the probability that the frequency of a scattered photon is shifted by a factor t, one can express the scattered spectrum as

$$j(x) = \int_0^\infty dt\, P(t)\, i(x/t)\,, \tag{15}$$

where $P(t)$ gives the probability that a photon is scattered to a frequency t times its original frequency. For a given electron spectrum $f_{\rm e}(p)\,dp$, where $p = \beta_{\rm e}\,\gamma_{\rm e}$ is the normalized electron momentum, and where $\int dp\, f_{\rm e}(p) = 1$, the photon redistribution function can be written as

$$P(t) = \int_0^\infty dp\, f_{\rm e}(p)\, P(t;p)\,. \tag{16}$$

$P(t;p)$ is the redistribution function for a momoenergetic electron distribution. $P(t;p)$ can be derived following Wright's (1979) kinematical considerations of the IC scattering in the Thomson regime ($h\,\nu \ll \gamma_{\rm e}\,m_{\rm e}\,c^2$). Scattering of a photon from an isotropic photon field has a probability distribution of the angle θ between photon and electron direction in the electron's rest frame given by

$$f(\mu)\,d\mu = [2\gamma_{\rm e}^4(1-\beta_{\rm e}\mu)^3]^{-1}\,d\mu\;, \tag{17}$$

where $\mu = \cos\theta$. The frequency shift from ν to ν' of the photon after scattering into an angle θ' is

$$t = \frac{\nu'}{\nu} = \frac{1+\beta_{\rm e}\mu'}{1-\beta_{\rm e}\mu}\,. \tag{18}$$

The probability distribution of $\mu' = \cos\theta'$ for a given μ is

$$g(\mu';\mu)\,d\mu' = \frac{3}{8}[1+\mu^2\mu'^2+\frac{1}{2}(1-\mu^2)(1-\mu'^2)]\,d\mu' \tag{19}$$

(Chandrasekhar 1950). The probability for a shift t given the electron velocity is

$$P(t;p) = \int d\mu\, f(\mu)\, g(\mu';\mu)\,\left(\frac{\partial\mu'}{\partial t}\right)\,. \tag{20}$$

$\mu'(t,\beta_{\rm e},\mu)$ is given by (18) and the range of integration is given by the conditions $-1<\mu<1$ and $-1<\mu'<1$. The integrand in (20) is a rational function of μ and therefore analytically integrable:

$$P(t;p) \;=\; -\frac{3|1-t|}{32p^6t}\left[1+(10+8p^2+4p^4)t+t^2\right] \tag{21}$$

$$+\;\frac{3(1+t)}{8p^5}\left[\frac{3+3p^2+p^4}{\sqrt{1+p^2}}\right. \tag{22}$$

$$\left.-\;\frac{3+2p^2}{2p}(2\,\mathrm{arcsinh}(p)-|\ln(t)|)\right]$$

The maximal frequency shift is given by

$$|\ln(t)| \le 2\,\mathrm{arcsinh}(p)\,, \tag{23}$$

and therefore $P(t;p) = 0$ for $|\ln(t)| > 2\,\mathrm{arcsinh}(p)$. Similar expressions for the photon redistribution function using different variables can be found in the literature (Rephaeli 1995a; Fargion et al. 1996; Enßlin & Biermann 1998; Sazonov & Sunyaev 2000). We verified analytically, that $P(t;p)$ has the proper normalization ($\int dt\, P(t;p) = 1$) and checked numerically that it also reproduces the known average energy gain of the scattered photons ($\int dt\, P(t;p)\,(t-1) = \frac{4}{3}\,p^2$).

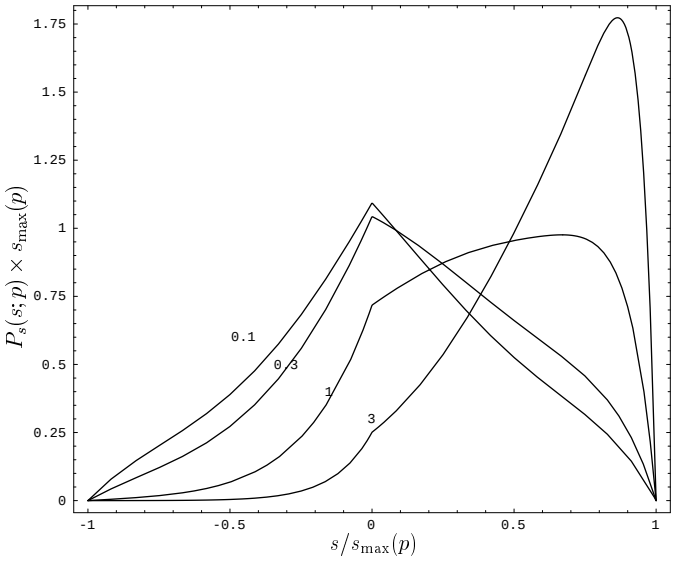

Fig. 2. The frequency redistribution function $P_s(s)$ plotted in normalized coordinates ($P_s(s;p) \times s_{\max}(p)$ over $s/s_{\max}(p)$) for different electron momenta p. From the left to the right curve is $p = 0.1, 0.3, 1, 3$, yielding $s_{\max}(p) = 0.2, 0.6, 1.8, 3.6$ or $t_{\max}(p) = e^{s_{\max}(p)} = 1.2, 1.8, 5.8, 38$.

If one is interested in the large frequency shift ($t \gg 1$) due to IC-scattering by ultra-relativistic electrons it is convenient to use the logarithmic frequency shift $s = \ln(t)$. The photon redistribution function then reads

$$P_s(s;p)\, ds = P(e^s;p)\, e^s\, ds\,, \tag{24}$$

and $P_s(s;p) = 0$ for $|s| > s_{\max}(p) = 2\,\mathrm{arcsinh}(p)$. $P_s(s;p)$ is plotted in Fig. 2.

We are interested in three distinct forms of the momentum distribution of the scattering electrons:

– a thermal electron distribution:

$$f_{\mathrm{e,th}}(p;\beta_{\mathrm{th}}) = \frac{\beta_{\mathrm{th}}}{K_2(\beta_{\mathrm{th}})}\; p^2\; \exp(-\beta_{\mathrm{th}}\sqrt{1+p^2})\,, \tag{25}$$

with K_ν denoting the modified Bessel function of the second kind (Abramowitz & Stegun 1965), introduced here for proper normalization, and $\beta_{\mathrm{th}} = m_{\mathrm{e}}\, c^2/kT_{\mathrm{e}}$ the normalized thermal beta-parameter.

– a power-law distribution between p_1 and p_2, as a model for a cosmic ray (CR) electron population:

$$f_{\mathrm{e,cr}}(p;\alpha,p_1,p_2) = \frac{(\alpha-1)\,p^{-\alpha}}{p_1^{1-\alpha}-p_2^{1-\alpha}} \tag{26}$$

– a thermal distribution with a high-energy power-law tail, as a model for a thermal population modified by in-situ particle acceleration:

$$f_{\mathrm{e,th\&cr}}(p;\beta_{\mathrm{th}},\alpha,p_1,p_2) = C_{\mathrm{e}}(\beta_{\mathrm{th}},\alpha,p_1,p_2)\,\times \left\{ \begin{array}{lll} f_{\mathrm{e,th}}(p;\beta_{\mathrm{th}}) & ; & p \le p_1 \\ f_{\mathrm{e,th}}(p_1;\beta_{\mathrm{th}})\,(p/p_1)^{-\alpha} & ; & p_1 < p < p_2 \\ 0 & ; & p_2 < p \end{array} \right\}, \tag{27}$$

where the normalization parameter $C_{\mathrm{e}}(\beta_{\mathrm{th}},\alpha,p_1,p_2)$ is determined by $\int dp\, f_{\mathrm{e,th\&cr}}(p;\beta_{\mathrm{th}},\alpha,p_1,p_2) = 1$.

The integral in Eq. (16) has to be evaluated numerically for the thermal electron distribution. But the analytical solution for the power-law case can be expressed as

$$\begin{aligned} P_{\mathrm{cr}}(t;\alpha,p_1,p_2) &= \frac{\alpha-1}{p_1^{1-\alpha}-p_2^{1-\alpha}}\,\frac{3}{16}\,(1+t)\,\times \\ &\Bigg[-\mathrm{B}_{\frac{1}{1+p^2}}\left(\frac{1+\alpha}{2},-\frac{\alpha}{2}\right) \\ &-\mathrm{B}_{\frac{1}{1+p^2}}\left(\frac{3+\alpha}{2},-\frac{2+\alpha}{2}\right)\,\frac{7+3\,\alpha}{3+\alpha} \\ &-\mathrm{B}_{\frac{1}{1+p^2}}\left(\frac{5+\alpha}{2},-\frac{4+\alpha}{2}\right)\,\frac{12+3\alpha}{5+\alpha} \\ &+p^{-5-\alpha}\left\{\left(\frac{3}{5+\alpha}+\frac{2\,p^2}{3+\alpha}\right)\,(2\,\mathrm{arcsinh}(p)-|\ln(t)|)\right. \\ &\left.+\left|\frac{1-t}{1+t}\right|\,\left(\frac{1+t^2}{2(5+\alpha)t}+\frac{5}{5+\alpha}+\frac{4\,p^2}{3+\alpha}+\frac{2\,p^4}{1+\alpha}\right)\right\}\Bigg]_{\tilde{p}_1(t)}^{\tilde{p}_2(t)}, \end{aligned} \tag{28}$$

with $\tilde{p}_1(t) = \max(p_1, \sqrt{t}/2)$ and $\tilde{p}_2(t) = \max(p_2, \sqrt{t}/2)$. Here $\mathrm{B}_x(a,b)$ denotes the incomplete beta-function (Abramowitz & Stegun 1965), and

$$[f(p)]_{p_1}^{p_2} = f(p_2) - f(p_1)\,. \tag{29}$$

$P_{\mathrm{cr}}(t;\alpha,p_1,p_2) = 0$ if $|\ln(t)| > 2\,\mathrm{arcsinh}(p_2)$. This function is plotted in Figs. 3 and 4. The resulting change in a blackbody photon spectrum due to Comptonization by CR-electrons is shown in Fig. 1 as the curves labeled with $j-i$. Note that for a given frequency the influence of the gain in up-scattered photons of lower initial frequencies, $j_{\mathrm{cr}}(x)$, on the spectral distortions are negligible compared to $-i(x)$, which describes the loss of photons from the CMB of intially this frequency, as long as $x < 10$ and the lower cutoff the electron spectrum $p_1 > 3$. Therefore the rSZ effect can be well approximated as a pure absorption process of photons in the CMB-spectral range ($x < 10$) for sufficiently relativistic electrons, justifying Eq. (1).

3.2. Relativistic SZ-effect in emission

Above the crossover frequency ($x_{\mathrm{cross}} \geq 3.83$) the arriving up-scattered photons outnumber the disappearing ones giving an SZ increment. This has a different spectral shape in the relativistic case compared with the classical one. The higher the frequency, the stronger is the rSZ effect compared to the thSZ effect. This provides for a promising opportunity to detect rSZ effect via this characteristic signature. Figs. 5 – 7 illustrate this. A direct application of the emission signature of the rSZ effect can be found in Sect. 5.2.

4. Radio galaxies

4.1. Remnant radio plasma

The presence of radio plasma produces all three SZ effects discussed in this paper: The expanding lobes of radio galaxies

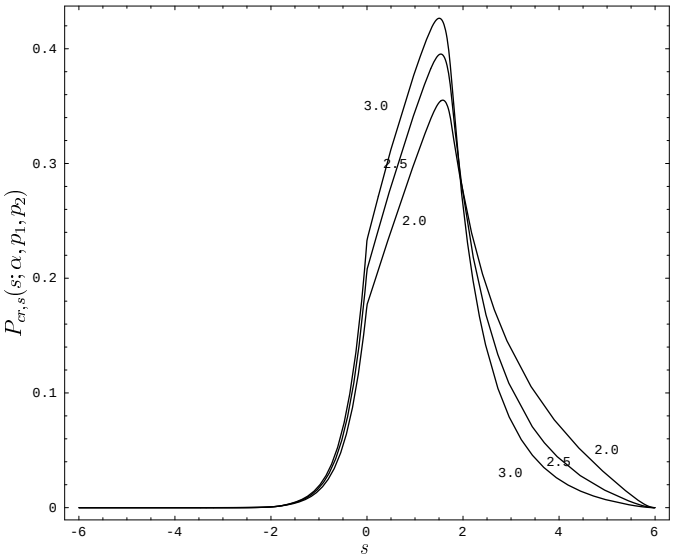

Fig. 3. The CR-frequency redistribution function $P_{\rm cr,s}(s;\alpha,p_1,p_2)$ over s. $p_1 = 1$, $p_2 = 10$, and $\alpha = 3.0, 2.5, 2.0$ from left to right.

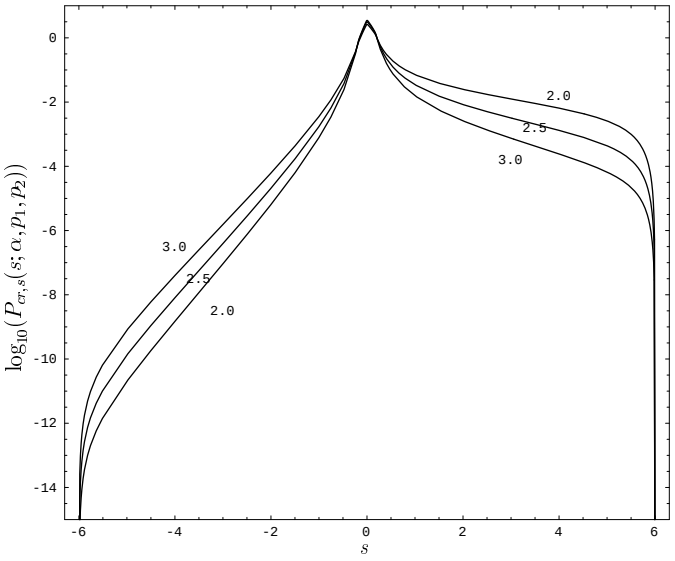

Fig. 4. The CR-frequency redistribution function in logarithmic units $\log_{10}(P_{\rm cr,s}(s;\alpha,p_1,p_2))$ over s. $p_1 = 0.1$, $p_2 = 10$, and $\alpha = 3.0, 2.5, 2.0$ from left to right.

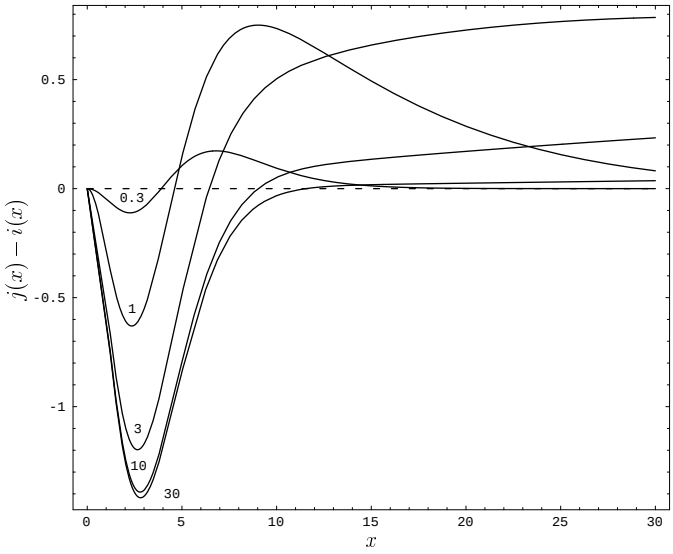

Fig. 5. $j(x) - i(x)$ for mono-energetic electron spectra with $p = 0.3$, 1, 3, 10, 30. These curves give the spectral change per electron of this momentum. Note that the absorption feature saturates to $-i(x)$ for $p \geq 10$.

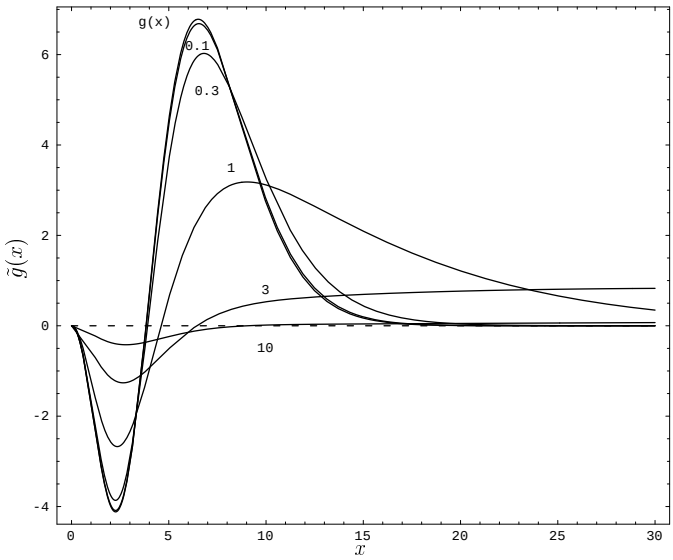

Fig. 6. The relativistically correct $\tilde{g}(x)$ for mono-energetic electron spectra with $p = 0.1$, 0.3, 1, 3, 10. Also the low energy limit $g(x)$ is shown, which is the curve with the most pronounced extrema. The curves are proportional to the spectral change per electron pressure.

(RGs) and radio-loud quasars compress and may shock the ambient IGM, thereby increasing its thSZ effect. During the inflation phase of the radio lobes the ambient medium is pushed aside, leading to a possible kSZ effect. And finally the relativistic electron content of the radio plasma produces the rSZ effect.

The inflation phase of a RG is short compared to cosmological times, thus we do not consider the transient kinematic effect. Furthermore, since gas on both sides of the radio lobes is accelerated in different directions, giving contributions of opposite sign but similar strength which should therefore roughly cancel out. In Sect. 4.3 we argue that the combined kSZ effect of an isotropic ensemble of flows is practically indistinguishable from a thSZ effect with the same energy content, further justifying our simplified treatment.

Radio lobes become unobservable due to adiabatic, IC- and synchrotron energy losses of the electrons on a time-scale shorter than the expansion time of the radio lobes which leads to pressure equilibrium with the surrounding medium (e.g. Kaiser et al. 2000). However, the energy transfered to the IGM by the expansion of the lobes, and also the relativistic electron population remain and leave their fingerprints in the CMB spectrum via Comptonization.

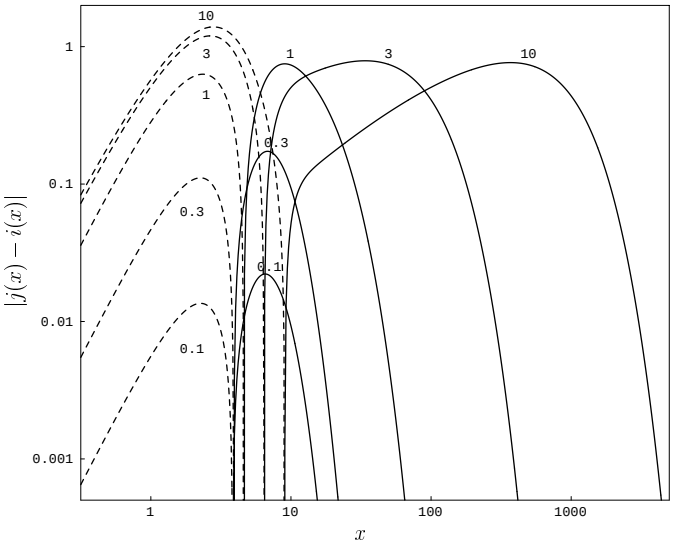

Fig. 7. $|j(x) - i(x)|$ for mono-energetic electron spectra in double logarithmic units. The dashed lines show absorption, the solid lines emission. The curves are labeled with the electron momentum.

The radio plasma and later radio ghosts will expand or contract until they reach pressure equilibrium with the surrounding medium. The pressure of the radio ghost is given by that of the confined relativistic particles and the magnetic fields, assumed to be in rough energy equipartition. Thus the magnetic field energy densities should be of the order of the thermal energy density of the environment. Subsonic turbulence in this environment, which has an energy density below the thermal energy density, is therefore not strong enough to overcome the magnetic elastic forces of the radio ghost if the magnetic field in the ghost is contiguous on large scales. In the case of a magnetic field disjoined on scales smaller than the physical size of the ghost and/or the turbulence being sonic or super-sonic, which is e.g. expected in giant merger events of cluster of galaxies, it can 'shred' the ghost into smaller pieces. The size of such pieces will be comparable to the eddy size of the turbulence. This means, since a typical turbulent spectrum has less energy density on smaller scales, that there is a length-scale below which the turbulence is not able to overcome magnetic forces. Turbulent erosion of radio ghosts should stop at this length-scale, leaving small-scale patches of still unmixed old radio plasma. Similarly, fluid instabilities of Kelvin-Helmholtz or Rayleigh-Taylor type at the surface of the ghost will not lead to a complete mixing of the radio plasma with the surrounding matter.

The relativistic electrons suffer from adiabatic losses during the inflation phase of the radio plasma, afterwards only from synchrotron and IC- losses. Coulomb- and bremsstrahlung-losses are negligible in a tenuous relativistic plasma. The cooling of an ultra-relativistic electron with momentum p is governed by

$$-\frac{dp}{dt} = a_{\rm C} + a_{\rm b} p + a_{\rm s} p^2. \quad (30)$$

(Kardashev 1962), where we ignored adiabatic losses or gains due to volume changes. The coefficient $a_{\rm C}$, $a_{\rm b}$, and $a_{\rm s}$ for Coulomb, bremsstrahlung, and synchrotron/IC losses are (Rephaeli 1979, Blumenthal & Gould 1970)

$$a_{\rm C} = \frac{3}{2}\sigma_{\rm T}\, c\, n_{\rm e} \left(\ln \frac{m_{\rm e} c^2 p^{1/2}}{\hbar \omega_{\rm p}} + 0.22 \right), \quad (31)$$

$$a_{\rm b} = \frac{3\alpha}{\pi}\sigma_{\rm T}\, c\, n_{\rm e} \left(\ln 2p - \frac{1}{3} \right), \quad (32)$$

$$a_{\rm s} = \frac{4}{3}\frac{\sigma_T\, c}{m_{\rm e}\, c^2}\, (\varepsilon_{\rm B} + \varepsilon_{\rm cmb}), \quad (33)$$

where the electron density of the background gas is $n_{\rm e}$, $\varepsilon_{\rm B} = B^2/(8\,\pi)$ is the magnetic field and $\varepsilon_{\rm cmb}$ the CMB photon energy density. The plasma frequency is $\omega_{\rm p} = \sqrt{4\pi e^2 n_{\rm e}/m_{\rm e}}$ and α is the fine-structure constant. In order to judge the importance of the different terms in Eq. (30) we define the cooling times

$$t_{\rm C} = \frac{p}{a_C} = 22\,{\rm Gyr}\ \ (1 + 0.01\ \ln(p_1/n_{-5}))^{-1}\ p_1/n_{-5}, \quad (34)$$

$$t_{\rm b} = \frac{1}{a_b} = 8.6 \cdot 10^3\,{\rm Gyr}\ \ (1 + 0.38\ \ln(p_1))^{-1}\ /n_{-5}, \quad (35)$$

$$t_{\rm s} = \frac{1}{a_s\, p} = 9.8\,{\rm Gyr}\ /(\varepsilon_{-11}\, p_1), \quad (36)$$

where $p_1 = p/10$, $n_{-5} = n_{\rm e}/(10^{-5}\,{\rm cm}^{-3})$, and $\varepsilon_{-11} = (\varepsilon_{\rm B} + \varepsilon_{\rm cmb})/(10^{-11}\,{\rm erg\,cm}^{-3})$. We note, that in the following estimates the radio plasma is assumed to contain relativistic electrons only above $p = 10$. From these timescales it becomes obvious that as long as the electron density within the radio plasma stays below $10^{-5}\,{\rm cm}^{-3}$ only synchrotron and IC losses have to be taken into account. If the radio plasma does not mix on a microscopic scale with the ambient medium this can be expected. In the following we assume that this is indeed the case. We note that in the case of a cold denser gas component in the radio plasma the Coulomb cooling heats the cold electron and this heat contributes to the thSZ-effect. The evolution of the relativistic electron distribution function in this case can be calculated analytically for constant conditions in the plasma ($B, n_{\rm e}, \varepsilon_{\rm cmb} = const$) (Enßlin et al. 1999). If Coulomb- and bremsstrahlung-cooling can be neglected Eq. (30) is solved by

$$p(t) = \left[\frac{1}{p_0} + \frac{4}{3}\frac{\sigma_T\, c}{m_{\rm e}\, c^2} \left(\frac{\langle B^2 \rangle}{8\,\pi} + \langle \varepsilon_{\rm cmb} \rangle \right) t \right]^{-1}, \quad (37)$$

where the brackets ($\langle ... \rangle$) indicate time-averaged quantities, and p_0 is the momentum at $t = 0$. In order to demonstrate that even under disadvantageous conditions electrons stay relativistic we insert $p_0 = 10$, $\langle B^2 \rangle = (20\,\mu{\rm G})^2$, and $\langle \varepsilon_{\rm cmb} \rangle = 11\,\varepsilon_{\rm cmb,today}$ corresponding to an time-average over the CMB energy density between today and $z = 2$ in an EdS Universe. The final electron momentum after $t = 10$ Gyr cooling is still $p > 3$. Thus, practically all relativistic electrons in old radio plasma stay relativistic for cosmological times. Their energies change, but this is not important for the rSZ effect in the spectral region of the CMB: the rSZ decrement depends practically only on the number of relativistic electrons, and not on their energy. This is because all the up-scattered photons have energies far above

the CMB range, so that their actual energy does not influence measurements within this range ($x < 10$). However, a search for up-scattered photons is a promising way to detect the rSZ-effect of very low energy relativistic electrons.

4.2. Detectability of radio ghosts

Beside the possibility to see a rSZ signature, discussed in this article, there are a few other possibilities to detect radio ghosts.

Radio ghosts are practically unobservable as long as their electron population remains at low energies. But if the population is re-accelerated the ghost becomes radio luminous again. This can happen when the ghost is dragged into a large-scale shock wave, e.g. in a merger event of clusters of galaxies or at the accretion shock where the matter is falling onto a cluster. The emission region is expected to be irregularly shaped, and should exhibit linear polarization due to the compression of the magnetic fields in the shock. Such regions are indeed observed in the periphery of a few clusters of galaxies and are called 'cluster radio relics' (for reviews, see Jaffe 1992 and Feretti & Giovannini 1996). Their properties, such as degree and direction of polarization, surface luminosity, peripheral position etc., can be understood within such a scenario (Enßlin et al. 1998a). The observed rarity of the cluster radio relic phenomena can be understood in this context: the presence of a shock wave, which should be quite frequently found in and near clusters of galaxies, is not sufficient to produce a cluster radio relic, a radio ghost has to be present at the same location, too.

Another way to detect the presence of radio ghosts is via their ability to magnetically scatter ultra-high energy (UHE) cosmic rays (CR) (Enßlin 1999). Without such scattering the distribution of sky arrival directions of UHE CR should trace their source distribution within ≈ 50 Mpc, due to the limited distance protons above $3 \cdot 10^{19}$ eV can travel without strong photo-pion energy losses (Greisen 1966, Zatsepin & Kuzmin 1966). If the distribution of UHE CR sources follows that of the matter in the local Universe a non-uniform arrival direction distribution is expected, contrary to the observations. Medina Tanco & Enßlin (in preparation) show that under optimistic assumptions about their distribution radio ghosts can sufficiently isotropize the UHE CR arrival directions. Since the UHE CR scattering angle decreases with particle energy, this scenario can in principle be tested, as soon as sufficient CR data is available.

4.3. The energy budget of radio ghosts

The energy a radio galaxy release into a radio ghost and its environment during its lifetime is

$$E_{\rm gh} = \varepsilon_{\rm gh}\, V_{\rm gh} + P\, V_{\rm gh} \tag{38}$$

where $V_{\rm gh}$ is the volume occupied by the ghost, P the pressure inside and outside the ghost and

$$\varepsilon_{\rm gh} = \varepsilon_{\rm e} + \varepsilon_{\rm p} + \varepsilon_B = (1 + k_p + k_B)\varepsilon_{\rm e} \tag{39}$$

is the energy density in the remnant radio plasma, split into its leptonic ($\varepsilon_{\rm e}$), hadronic ($\varepsilon_{\rm p}$) and magnetic (ε_B) part. Unfortunately, the ratios between these energy densities are still undetermined. The parameters $k_p = \varepsilon_p/\varepsilon_e$ and $k_B = \varepsilon_B/\varepsilon_e$ take account of this.

The radio plasma is expected to follow a relativistic equation of state ($P = \frac{1}{3}\varepsilon_{\rm gh}$; note that isotropically oriented magnetic fields also follow a relativistic equation of state). The fraction of $E_{\rm gh}$ stored as volume work in the ambient medium is therefore

$$\Delta E_{\rm th} = P\, V_{\rm gh} = \frac{1}{4}\, E_{\rm gh}\,. \tag{40}$$

This thermal energy produces a thSZ effect in addition to that expected from the heat in the IGM due to structure formation. It seems to be difficult to follow this energy in an expanding Universe with ongoing structure formation. But it can be argued that this energy is released into gravitationally bound structures (clusters and filaments of galaxies). Filaments expand due to the Hubble flow, but the matter within a given filament flows into the next galaxy cluster and gets compressed thereby. This means, that on a longer time-scale the extra heat from RG is expected to be confined in clusters of galaxies and does not suffer from adiabatic losses.

In fact, part of the energy injected into the environment might also be stored gravitationally whenever gas is pushed to a higher gravitational potential or transformed to kinetic energy of gas flows. Gravitational energy is converted to kinetic energy, whenever the accelerated gas flows into the next potential well. From Eqs. (1) and (6) one would conclude that the kSZ effect is zero for an average of isotropically oriented flows. But Eq. (1) is only an approximation. A better description of the average kSZ effect for an isotropic ensemble of flows can be gained by the following argument: the individual electron velocities of all flows measured in the CMB-rest frame can be combined into a single momentum space distribution function, which is of course isotropic. This function can be used in order to calculate the Comptonization with the formalism described in Sect. 3.1, since the latter does not depend on the position of an electron along the line of sight in the optically thin limit. The kinetic energies are non-relativistic, so that the spectral changes are well described by the function $g(x)$ times the total kinetic energy of the electrons (see Fig. 6). Thus the Comptonization is independent of the exact spectral shape of the electron spectrum or the distribution of flow velocities. Therefore we assume that all of the energy, which the inflating radio lobes give to their environment, contributes to the thSZ effect. A similar argumentation for gaussian, isotropic, random velocity fields was given in Zeldovich et al. (1972).

We approximate the relativistic electron spectrum by a single power-law (Eq. (27)), so that the energy density $\varepsilon_{\rm e}$ and the number density $n_{\rm e,cr}$ of the relativistic electron of a ghost are related via the average kinetic energy of the electrons ($\langle\gamma_{\rm e} - 1\rangle\, m_{\rm e}\, c^2$):

$$\varepsilon_{\rm e} = n_{\rm e,cr}\, \langle\gamma_{\rm e} - 1\rangle\, m_{\rm e}\, c^2 \approx \frac{\alpha - 1}{\alpha - 2}\, n_{\rm e,cr}\, m_{\rm e}\, c^2\, p_1\,. \tag{41}$$

The approximation assumes the particles to be ultra-relativistic ($1 \ll p_1 < p_2$) and the distribution to be dominated by the

lower end ($p_1 \ll p_2$ and $\alpha > 2$). In the case that the distribution has a trans- or non-relativistic part the exact formulae for energy density, pressure and adiabatic index can be found in Appendix A.

If the ultra-relativistic approximation is valid and the low energy electrons dominate the spectrum, we can write:

$$n_{\rm e,cr} = \frac{\alpha-2}{\alpha-1}\,\frac{\varepsilon_{\rm gh}}{(1+k_{\rm p}+k_B)\,m_{\rm e}\,c^2\,p_1}\,. \quad (42)$$

All the quantities on the rhs have to be inserted for the same stage of the radio plasma evolution in order to give a consistent result. The best observational constraints for these quantities are of course given for the moment of injection, when the radio plasma is visible.

4.4. CMB-distortions

We estimate now the Comptonization due to energy from radio galaxies stored in different forms into the IGM. We have to calculate the integrals in Eqs. (4) and (7) in a cosmological context. We need to know the distribution of injected heat and relativistic electrons. Since both quantities (injected thermal heat in the IGM and number of relativistic electrons in the radio plasma) are accumulative in the sense, that radio galaxies produce them, but cooling mechanisms are insufficient to remove them. For the thermal energy this is clear, since except for cooling flows in the very center of some cluster of galaxies the cooling time exceeds the Hubble time. For the number density of relativistic electrons this follows from the fact that the dominant cooling mechanism in a tenuous relativistic plasma are synchrotron- and IC-cooling, which become inefficient for low energy electrons (see Sec 4.1).

The integrands in Eqs. (4) and (7) are proportional to the amount of remnant radio plasma at a given epoch (e.g. measured by the number density of relativistic electrons $n_{\rm e,rel}$). Since, as we argued, radio plasma is conserved, its electron density is given by

$$n_{\rm e,rel}(t) = \int_0^t dt'\,\dot{n}_{\rm e,rel}(t')\,, \quad (43)$$

where $\dot{n}_{\rm e,rel}(t)$ is the source electron density of radio plasma at time t in comoving coordinates. The optical depth of relativistic plasma can then be written as

$$\tau_{\rm rel} = \sigma_{\rm T}\,c\int_0^{z_{\rm max}} dz\,\frac{dt}{dz}\dot{n}_{\rm e,rel}(z)\int_0^z dz'\,\frac{dt}{dz'}\,(1+z')^3\,, \quad (44)$$

where $t(z)$ is the time between today and redshift z, and $z_{\rm max}$ is the maximal redshift of injection. We use $z_{\rm max}=4$, which is sufficiently low so that cooling effects can be neglected. Since $\dot{n}_{\rm e,rel}(z)$, the source density of relativistic electrons, is only poorly constrained observationally, we use $Q_{\rm jet}(t)$, the source density of energy from RG instead. For convenience, we define

$$\omega_{\rm gh} = \frac{\sigma_{\rm T}\,c}{m_{\rm e}\,c^2}\int_0^{z_{\rm max}} dz\,\frac{dt}{dz}\dot{Q}_{\rm jet}(z)\int_0^z dz'\,\frac{dt}{dz'}\,(1+z')^3\,, \quad (45)$$

and the total amount of energy release through radio plasma:

$$\bar{\epsilon}_{\rm gh} = \int_0^{z_{\rm max}} dz\,\frac{dt}{dz}\dot{Q}_{\rm jet}(z)\,. \quad (46)$$

For an ultra-relativistic and steep electron population inside ghosts the approximation Eq. (42) gives

$$\tau_{\rm gh} = \frac{3}{4}\,\frac{\alpha-2}{\alpha-1}\,\frac{\omega_{\rm gh}}{(1+k_{\rm p}+k_B)\,p_1}\,. \quad (47)$$

A similar expression gives the additional thSZ effect due to IGM heating by expanding radio lobes:

$$y_{\rm gh} = \frac{\omega_{\rm gh}}{12}\,. \quad (48)$$

This follows from Eq. (40) if we assume that the IGM protons get half of the heat energy.

The optical depth of radio ghosts can be written as

$$\tau_{\rm gh} = \frac{\alpha-2}{\alpha-1}\,\frac{9\,y_{\rm gh}/p_1}{(1+k_{\rm p}+k_B)} = \frac{y_{\rm gh}}{10}\,\frac{3}{1+k_{\rm p}+k_B}\,\frac{10}{p_1}\,. \quad (49)$$

Here, we inserted $\alpha = 2.5$. If we assume protons, electrons and magnetic fields to have all the same energy density, and insert a speculative lower electron cutoff of $p_1 = 10$, this equation suggests that $y_{\rm gh} \gg \tau_{\rm gh}$. This means that the thSZ decrement due to the thermal IGM heating by inflating radio lobes always dominates over the rSZ decrement of the relativistic electron population in these radio lobes since $|g(x)| \gg |i(x)|$ in the Rayleight-Jeans regime (see Fig. 1 and Eq. (1) for details). The thSZ increment in the Wien-regime decreases exponential and therefore much faster than the rSZ increment of a power-law electron population. Therefore the rSZ effect of radio plasma dominates over its induced thSZ effect at sufficiently high frequencies as long as the electron population stays relativistic.

The total jet power of radio galaxies per comoving volume can be derived from the radio luminosity function of RG with the additional assumption that there is a unique relation between radio luminosity and jet power. This is not strictly correct, since it is known that for the largest part of the observed lifetime of RGs they should exhibit some luminosity evolution, even in models with constant jet power (for the case of powerful RG of type FRII see e.g. Begelman & Cioffi 1989, Falle 1991, Kaiser & Alexander 1997, Kaiser et al. 1997, Daly 1999). But this evolution is 'modest' (roughly an order of magnitude) and its influence should produce some scatter in an empirical derived relation, but not a large systematic effect. Similarly we neglect the influence of the density of the gas in the radio source environments on its radio luminosity. Again we expect this only to increase the scatter about the empirical function we will use in the following to relate radio luminosity and jet power.

Enßlin et al. (1997) have fit a power-law to the jet power – radio luminosity relation derived by Rawlings & Saunders (1991) for a sample of radio galaxies, which includes both, the most powerful radio galaxies of type FRII and also the somewhat less luminous FRI objects. Their results are based on minimum energy arguments and age estimates. The real energy of radio plasma can easily be much higher than the minimal

energy estimate by some factor $f_{\rm power} > 1$ due to the presence of relativistic protons, low energy electrons or deviations from equipartition between particle and field energy densities. A rough estimate of $f_{\rm power}$ can be derived from observations of radio lobes embedded in the intra-cluster medium (ICM) of clusters of galaxies. These observations show a discrepancy of the thermal ICM-pressure to the pressure in the radio plasma following minimal energy arguments of a factor of $5-10$, even if projection effects are taken into account (e.g. Feretti et al. 1992). Since also a filling factor smaller than unity of the radio plasma in the radio lobes can mimic a higher energy density we chose $f_{\rm power} = 3$ in order to be conservative.

The jet power – radio luminosity correlation at $\nu = 2.7\,$GHz is

$$q_{\rm jet}(L_\nu) = a_\nu \, (L_\nu/(\mathrm{Watt\,Hz^{-1}}\, h_{50}^{-2}))^{b_\nu} \, f_{\rm power} \qquad (50)$$

for which $b_\nu = 0.82 \pm 0.07$, $\log_{10}(a_\nu/\mathrm{erg\,s^{-1}}\, h_{50}^{-2}) = 45.28 - 26.22 \cdot b_\nu \pm 0.18$ (Enßlin et al. 1997). This relation allows to integrate the observed radio luminosity function $n_\nu(L_\nu, t)$ in order to get the total jet power

$$Q_{\rm jet}(z) = \int_{L_{\rm min}}^{L_{\rm max}} dL_\nu \, n_\nu(L_\nu, z) \, q_{\rm jet}(L_\nu)\,. \qquad (51)$$

We use $L_{\rm min} = 10^{23}\,\mathrm{Watt\,Hz^{-1}}$, which is just above the region of the RLF which is dominated by starburst galaxies, and $L_{\rm max} = 10^{29}\,\mathrm{Watt\,Hz^{-1}}$. We adopt different radio-luminosity functions parameterized by Dunlop & Peacock (1990) and integrate Eq. (51) in an EdS-cosmology up to redshift $z_{\rm max} = 4$. Strictly, the expressions for $n_\nu(L_\nu, t)$ used here only apply to those members of the radio source population with steep radio spectra (spectral index -0.7 or less). However, the space density of the flat spectrum population, which is thought to consist mainly of FRI-type objects, is at least a factor 10 smaller at any given redshift (Dunlop & Peacock 1990). Therefore we can safely neglect their contribution to the overall radio luminosity function. We further calculate the ghost distribution function for $b_\nu = 0.7, 0.82, 1$ in order to show the dependence on the uncertainties.

Results of the integration of the different RLFs and jet power-radio luminosity correlations are given in Table 1. The energy input in form of radio plasma is roughly $\bar\epsilon_{\rm gh} = 3 \cdot 10^{66}\,\mathrm{erg\,Gpc^{-3}}\,(f_{\rm power}/3)$.

Note that the X-ray background, which is believed to be dominated by AGN emission, corresponds to an injection energy of $10^{67-68}\,\mathrm{erg\,Gpc^{-3}}$ in comoving coordinates (Soltan 1982; Chokshi & Turner 1992; Fabian & Iwasawa 1999; Fabian 1999). Either the X-ray energy losses of AGNs exceed the radio plasma release, or if X-ray power is comparable to the jet power then the latter is strongly underestimated here and $f_{\rm power} \approx 30$ would be more realistic. The resulting Comptonization would be comparable to the present-day upper limit of $y < 1.5 \cdot 10^{-5}$ (Fixsen et al. 1996). The extra-galactic radio background has an energy density of $\approx 5 \cdot 10^{63}\,\mathrm{erg\,Gpc^{-3}}$ (Longair & Sunyaev 1971), which is several orders of magnitude below the energy density in the X-ray background and the expected ghost energy density. This indicates that radio emission is a very inefficient mechanism to extract energy from radio plasma.

Table 1. Cosmological energy output of radio galaxies for two radio luminosity functions of Dunlop & Peacock (1990) and expected Comptonization parameter (Eq. (48)). PLE denotes the pure luminosity evolution and RLF2 is the second free-form model of Dunlop & Peacock. The optical depth $\tau_{\rm gh}$ of the relativistic electrons in ghosts is not well determined since it depends on several unknown parameters. Eq. (49) should be used in order to translate $y_{\rm gh}$ to $\tau_{\rm gh}$. If the internal energy of the radio plasma is fully thermalized, then $y_{\rm gh}$ increases by a factor of up to 4.

RLF	b_ν	$\bar\epsilon_{\rm gh}$	$y_{\rm gh}$
		$10^{66}\,\mathrm{erg\,Gpc^{-3}}$	10^{-6}
PLE	0.7	2.80	1.51
PLE	0.82	2.19	1.23
PLE	1.0	1.91	1.15
RLF2	0.7	4.86	1.94
RLF2	0.82	3.04	1.40
RLF2	1.0	2.04	1.18

It is interesting to note that the X-ray background predicts a mass density in AGN black holes of $(1.4...2.2)\cdot 10^{14}\,M_\odot\,\mathrm{Gpc^{-3}}$ for a mass-to-light-conversion-efficiency of AGNs of 0.1. This is consistent with the central black hole mass density derived from the observed black-hole-to-galactic-bulge-mass ratio and the observed masses of galaxies (Faber et al. 1997).

If the total energy of the radio lobes would be thermalized, then no rSZ-effect would result, but the contribution to the thSZ effect would increase by a factor of 4, shifting it closer to the present upper limit.

4.5. Discussion

The expected thermal Comptonization due to heating of the environment of RG is of the order of $y = 1.4 \cdot 10^{-6}\,(f_{\rm power}/3)$, if it is assumed that radio ghosts do not thermalize their internal energy, otherwise up to a factor of 4 higher. $f_{\rm power}$ is the ratio of true energy over equipartition energy in radio lobes.

There are two attempts in the literature to estimate the thSZ effect due to energy release from RGs.

Enßlin et al. (1998b) give $y \leq 1.0 \cdot 10^{-5}\,\eta_{\rm jet/X-ray}$. For this estimate they assume that the jet power is completely thermalized, and that the energy budget is the same as the X-ray energy release ($\eta_{\rm jet/X-ray} \approx 1$, thus 10 times higher than what we estimate here). It was also assumed that the thermal energy suffers from adiabatic cooling due to the Hubble flow, but since radio galaxies are located in filaments and clusters of galaxies, only 1-dimensional instead of 3-dimentional expansion was taken into account.

Yamada et al. (1999) use a model for heating and cooling of the environment of radio lobes. They estimate the jet power from the black-hole-to-galaxy mass ratio ($f_{\rm bh} = 0.002$) using a Press-Schechter description of galaxy (and black hole) growth and assuming a constant fraction ($f_{\rm rg} = 0.01$) of galaxies above $10^{12}\,M_\odot$ to be active RGs. Since the total energy release in

their description should be higher by an order of magnitude, compared to what we estimate here, it is not surprising that they get $y = 5.7 \cdot 10^{-5}\,(f_{\rm bh}/0.002)\,(f_{\rm r}/0.01)$, which slightly violates the present day upper limit.

The present day limit on the Comptonization parameter gives already an important constraint on the energy budget of RGs, which will be improved in the near future. If it would be possible to detect the spectral signature of a rSZ effect, a further major step in the investigation of radio plasma could be achieved. We do not give detailed predictions for the rSZ increment, since different to the rSZ decrement at lower frequencies it strongly depends on the unknown shape of the electron distribution. But observations of the rSZ effect in emission could allow a spectral examination of the low-energy end of the relativistic electron content of the Universe.

5. Clusters of galaxies

5.1. Embedded radio plasma

Clusters of galaxies are known to be strong sources of the thSZ effect. Since the thermal gas causing the thSZ distortions can also be observed with X-ray satellites via its bremsstrahlung emission it is possible to compare the angular diameter with the true line-of-sight diameter of the cluster. This gives directly the Hubble parameter, H_0, assuming spherical symmetry at least in a statistical sense. It is therefore of principal interest to estimate the possible influence of relativistic plasma on the measured Comptonization.

Radio plasma was mostly produced by outflows from AGN in virialized cosmological structures such as filaments and clusters of galaxies. Subsequent flows into deeper gravitational potentials should have transported a significant fraction of all radio plasma into clusters of galaxies. If the radio plasma is still unmixed with the thermal medium, it resembles a cavity in the X-ray emitting ICM gas. We assume in the following that a (for simplicity constant) fraction $\Phi_{\rm gh}$ of the cluster volume is occupied by radio ghosts. The X-ray luminosity of this cluster is thus given by

$$L_X = a_X \int dV\, n_{\rm e}^2\, kT_{\rm e}^{\frac{1}{2}}\,(1-\Phi_{\rm gh}) \sim l_{\rm cl}^3\, n_{\rm e,0}^2\,(1-\Phi_{\rm gh})\,. \quad (52)$$

$n_{\rm e}$ is the cluster electron density, $n_{\rm e,0}$ its central value, and $l_{\rm cl}$ the characteristic length scale of the cluster (e.g the core radius). Since the cluster temperature $kT_{\rm e}$ can be determined spectroscopically we assume it to be known. The thSZ effect

$$y_{\rm cl} = \frac{\sigma_T}{m_{\rm e}\,c^2} \int dl\, n_{\rm e}\, kT_{\rm e}\,(1-\Phi_{\rm gh}) \sim l_{\rm cl}\, n_{\rm e,0}\,(1-\Phi_{\rm gh}) \quad (53)$$

in combination with Eq. (52) allows to measure the typical scale of the cluster:

$$l_{\rm cl} \sim \frac{L_X}{y_{\rm cl}^2}\,(1-\Phi_{\rm gh}) \quad (54)$$

Since the angular diameter of a cluster should (at least in a statistical average) be identical to $l_{\rm cl}$ the Hubble constant can be derived:

$$H_0 \sim l_{\rm cl}^{-1} \sim \frac{y_{\rm cl}^2}{L_X\,(1-\Phi_{\rm gh})}\,. \quad (55)$$

There are two ways the presence of radio ghosts can affect the determination of H_0, which shift it in opposite directions: First, if a significant fraction of the volume is filled with relativistic plasma, then the true H_0 is greater than the one derived under the assumption that $\Phi_{\rm gh} = 0$. Second, if the measured $y_{\rm obs}$ contains a significant contamination due to absorption by the rSZ effect the true $y_{\rm cl}$, and therefore also H_0, is lower.

The second effect is negligible for the following reason: The optical depth of the relativistic electrons of the ghosts can be written as

$$\tau_{\rm gh} = \frac{6\,\phi_{\rm gh}\,y_{\rm cl}}{(1+k_B+k_p)\,\langle\gamma_{\rm e}-1\rangle\,(1-\Phi_{\rm gh})}\,, \quad (56)$$

if we assume pressure equilibrium between ghosts and thermal plasma, and use Eqs. (41), (53), and A.8. Optimistic values for the unknown parameters of the old radio plasma ($1+k_B+k_p \approx 3$, $\langle\gamma_{\rm e}-1\rangle \approx 10$) give $\tau_{\rm gh} \approx 0.2\,\Phi_{\rm gh}\,y_{\rm cl}$. The rSZ decrement is roughly $-\tau_{\rm gh}\,i(x)$, or smaller. The observed, rSZ-contaminated y-parameter is therefore

$$y_{\rm obs} = y_{\rm cl} + \frac{-i(x)}{g(x)}\,\tau_{\rm gh} \approx y_{\rm cl}\,(1+0.06\,\phi_{\rm gh})\,. \quad (57)$$

In the last approximation we assumed that the measurement is taken around $x = h\,\nu/kT_{\rm cmb} \approx 2$, where the thSZ absorption is at its maximum and $-i(x)/g(x) \lesssim 0.3$ (see Fig. 1). Inserting $y_{\rm obs}$ instead of $y_{\rm cl}$ into Eq. (55) gives an systematic error of $\approx 0.1\,\Phi_{\rm gh}$, which is an order of magnitude smaller than the error due to the factor $1-\Phi_{\rm gh}$ in the denominator of that equation. The error due to the rSZ effect could be larger, if the measurement is done closer to the crossover frequency at $x = 3.83$. However, this value of x is inconvenient for detecting the thSZ effect. Also if $\langle\gamma_{\rm e}-1\rangle \approx 1$ the distortion would be significant, but this is extremely speculative.

We conclude that the presence of a significant fraction of the volume of the ICM filled by radio ghosts biases the determination of the Hubble constant to lower values, if this effect is not accounted for.

5.2. Non-thermal electrons in the ICM

In some clusters of galaxies a relativistic ICM population of electrons is visible due to their synchrotron emission, which produces the radio halos of clusters of galaxies. Also the recently detected extreme ultraviolet (EUV) excess (Lieu et al. 1996) and the high energy X-ray (HEX) excess (Fusco-Femiano et al. 1998, 1999) in the Coma cluster indicate the presence of non-thermal electrons.

Our knowledge about the slope of the electron spectrum in the ICM is limited (see Enßlin & Biermann 1998 for an attempt to compile the electron spectrum in the Coma cluster). The number density and therefore the optical depth of the higher energy

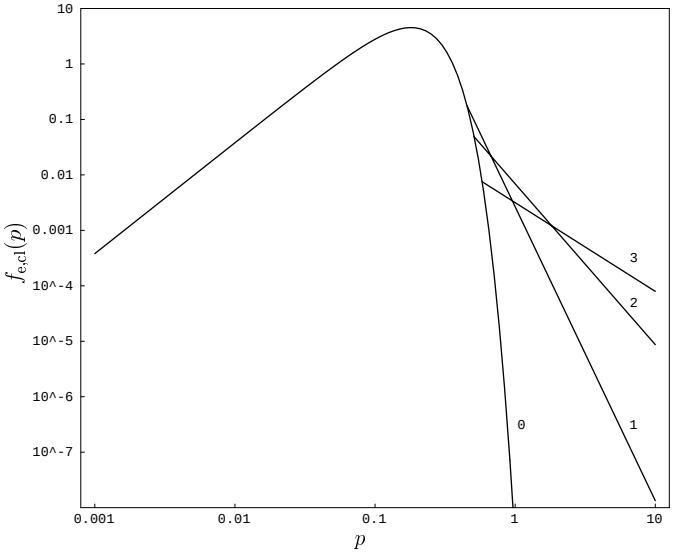

Fig. 8. The models 0-3 for the electron spectrum in Coma $f_{\rm e,cl}(p)$.

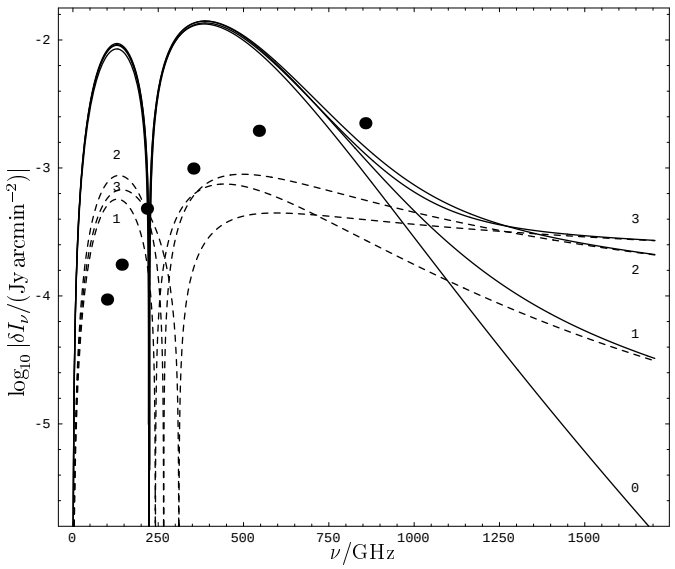

Fig. 9. $\log_{10}|\delta I_\nu/(\mathrm{Jy\,arcmin^{-2}})|$ over ν/GHz for the center of the Coma cluster. The solid lines are models 0-3 and the dashed lines are the difference of models 1–3 to model 0. The dots give the frequencies and sensitivities of single beams of the Planck satellite (Bersanelli et al. 1996; Puget 1998; see also Table 2). Since the angular diameter of Coma (core radius $\hat{=}10'$) is much larger than the beam of Planck (FWHM $\leq 10'$) a marginal detection (see Appendix B) of a possible non-thermal electron population producing the HEX excess by bremsstrahlung can be expected. Balloon experiments or other high-altitude observatories (at the planned ALMA site or in Antarctica) will be much more sensitive. Note that the curves on the lhs represent absorption, whereas the ones on the rhs represent emission.

electrons is too small to detect the rSZ decrement produced by them. See Birkinshaw (1999) for a discussion of the rSZ decrement from radio emitting electrons and McKinnon et al. (1991) for an attempt to detect this decrement in radio galaxies. The rSZ effect emission from these electrons may already have been observed in the EUV (Hwang 1997; Enßlin & Biermann 1998; Sarazin & Lieu 1998; Bowyer & Berghöfer 1998) or in the HEX excess (Fusco-Femiano et al. 1998, 1999). The latter would require a high number of electrons in the range of $3-5$ GeV, which would over-produce radio emission if the magnetic fields are as high as Faraday rotation measurements indicate ($2-10\,\mu$G; Crusius-Waetzel et al. 1990; Kim et al. 1991; Feretti et al. 1995, 1999; Clarke et al. in preparation). Only if fields are as weak as $0.16\,\mu$G consistency between the expected and observed radio flux is established (Fusco-Femiano et al. 1998, 1999). As a possible solution of this apparent contradiction of magnetic field estimates Enßlin et al. (1999) and Sarazin & Kempner (2000) proposed that the HEX excess could alternatively be produced by bremsstrahlung of a non-thermal high energy tail of the thermal electron distribution. Such a tail could exist due to in-situ particle acceleration powered by ICM turbulence (Enßlin et al. 1999; Dogiel 1999; Blasi 2000).

Detection of the IC emission of such a non-thermal tail could confirm the bremsstrahlung-scenario. In the following we estimate the expected spectral distortions for the Coma cluster of galaxies.

The electron density of the cluster is assumed to follow a beta-profile:

$$n_{\rm e}(r) = n_{\rm e,0}\,\left[1+(r/r_{\rm cl})^2\right]^{-\frac{3}{2}\,\beta_{\rm cl}}\,, \tag{58}$$

where $r_{\rm cl} = 400\,\mathrm{kpc\,h_{50}^{-1}}$ is the core radius, $\beta_{\rm cl} = 0.8$ is the beta-parameter, and $n_{\rm e,0} = 2.89\cdot 10^{-3}\,\mathrm{cm^{-3}}$ is the central thermal electron density (Briel et al. 1992). We ignore the possible complication due to embedded old radio plasma discussed in Sect. 5.1 for simplicity.

The optical depth of a line of sight passing the cluster center at a distance R is then

$$\tau_{\rm cl}(R) = \mathrm{B}\left(\frac{1}{2},\frac{3\,\beta_{\rm cl}-1}{2}\right)\,\frac{n_{\rm e,0}\,r_{\rm cl}\,\sigma_T}{\left[1+(R/r_{\rm cl})^2\right]^{\frac{3}{2}\,\beta_{\rm cl}-\frac{1}{2}}}\,, \tag{59}$$

giving a central optical depth of $\tau_{\rm cl}(0) = 5.95\cdot 10^{-3}$. The CMB-distortions are

$$\delta I_\nu = i_0\,\delta i(x) = i_0\,\tau_{\rm cl}\,(j(x)-i(x)))\,. \tag{60}$$

The electron spectrum is given for a thermal spectrum by Eq. (25) and for a modified thermal spectrum by Eq. (27). The non-thermal electrons are treated as an additional population, increasing slightly the total electron number, but leaving the number densities of electrons with $p < p_1$ unchanged. We estimate the distortions for a pure thermal spectrum (model 0) and for three modified thermal spectra, which are able to explain the HEX excess of Coma by bremsstrahlung (see Fig. 6 in Enßlin et al. 1999):

model 1: $\alpha = 5.3$, $p_1 = 0.45$, $E_{\rm kin,1} = 50\,\mathrm{keV}$;
model 2: $\alpha = 2.9$, $p_1 = 0.51$, $E_{\rm kin,1} = 62.5\,\mathrm{keV}$;
model 3: $\alpha = 1.6$, $p_1 = 0.58$, $E_{\rm kin,1} = 80\,\mathrm{keV}$;

$p_2 = 10$ in all three models. The electron spectra are shown in Fig. 8 and the resulting CMB distortions at the center of the Coma cluster in Fig. 9. The differences between the thermal and the modified thermal models are considerable and change

Table 2. The observing frequencies and sensitivities of the Planck satellite (Puget 1998). Note that the sensitivity $\Delta T/T$ refers to fluctuations in the radiation temperature, rather than to the system temperature of the receivers.

Channel k		1	2	3	4	5	6
Frequency ν_k	GHz	100	143	217	353	545	857
Frequency x_k		1.76	2.52	3.82	6.21	9.59	15.1
Beam FWHM$_k$	arcmin	10.7	8.0	5.5	5.0	5.0	5.0
Sensitivity $\Delta T/T$	$\mu K/K$	1.7	2.0	4.3	14.4	147	6670
Sensitivity $\Delta i(x_k)$	10^{-6}	4.09	7.66	21.0	43.2	85.2	97.6

as a function of frequency, so that future multichannel CMB telescopes such as high-altitude ground based observatories (e.g. at the ALMA site or in Antarctica), balloon-experiments, or marginally even the Planck satellite (see Appendix B) can discriminate between these models. A detection of this non-thermal SZ effect would prove in-situ acceleration processes acting in the ICM of Coma. It would confirm the bremsstrahlung origin of the HEX excess and therefore solve the discrepancy between Faraday and IC based magnetic field estimates in Coma.

Since the SZ effect does not depend on distance (as long as the instrument beam resolves the cluster core) many other clusters can be investigated for the presence of a non-thermal SZ effects with future CMB experiments.

6. Conclusion

We investigated the transrelativistic Thomson scattering of photons on a isotropic electron distribution in the optically thin limit using the photon redistribution kernel (Eq. (21)). We derived for the first time an analytic formula for the scattering by a population of electrons with a power law momentum distribution, Eq. (27). We demonstrated that relativistic electron populations produce a decrement in the cosmic microwave background, similar to that an absorber with an optical depth of the Thomson depth of the relativistic electrons would produce. Our formalism can be generalized to the optical finite case using the techniques described in Rephaeli (1995a,b) or Molnar & Birkinshaw (1999).

We applied this theory to radio galaxies and clusters of galaxies:

Although a single radio galaxy produces a negligible SZ decrement, the combined effect of several radio galaxies and their remnants might produce a detectable signal. In order to show this we estimated the total cosmological release in jet power of radio galaxies using the observed radio luminosity function converted by an empirical jet power-radio luminosity relation. It is roughly $3 \cdot 10^{66}\,\mathrm{erg\,Gpc^{-3}}\,(f_{\mathrm{power}}/3)$, where f_{power} gives the poorly constrained ratio between true energy content of radio lobes and the minimum energy estimate. If completely thermalized this energy would lead to a Comptonization parameter of $y \approx 6 \cdot 10^{-6}$, close to the present day observational limit of $y < 1.5 \cdot 10^{-5}$. We argued that roughly $3/4$ of the released energy remains as a relativistic plasma, which rapidly becomes unobservable after the activity of the galaxy stopped. Thus the Comptonization due to heating by radio plasma is expected to be $y \approx 1.5 \cdot 10^{-6}$.

Patches of old plasma, called 'radio ghosts', are expected to survive turbulent erosion unmixed with the ambient medium, so that they are able to retain a low energy relativistic electron population. The optical depth for Thomson scattering by radio ghosts is $\tau_{\mathrm{gh}} \approx 10^{-7}$ for very optimistic assumptions about the low energy cutoff of the fresh electrons during injection. Otherwise τ_{gh} is much lower.

If radio ghosts occupy a significant volume in clusters of galaxies, they affect the determination of the Hubble constant via SZ and X-ray measurements. The geometric effect of the cavities formed by ghosts in the intra-cluster gas overwhelms the SZ decrement expected due to up-scattering of CMB photons by the ghosts' relativistic electron populations. SZ based H_0 determinations have to be corrected to higher values due to this effect.

Finally, we demonstrated that future CMB telescopes such as the Planck satellite seemed to be useful tools to measure supra-thermal electron populations in clusters of galaxies. These are expected in the case of turbulent in-situ particle acceleration, and supported by the recently detected high energy X-ray excess in the Coma and Abell 2556 cluster. Such a detection would be crucial for our understanding of particle acceleration processes in clusters.

Acknowledgements. We thank Rashid Sunyaev, Matthias Bartelmann, and Mark Birkinshaw, the referee, for comments on the manuscript.

Appendix A: Energy density and pressure of a trans-relativistic power-law electron distribution

If an electron population, with number density $n_{\mathrm{e,cr}}$, has a momentum spectrum which is a single power-law (Eq. (27)) the kinetic energy density ε_{e} is

$$\varepsilon_{\mathrm{e}} = n_{\mathrm{e,cr}} \langle \gamma_{\mathrm{e}} - 1 \rangle m_{\mathrm{e}} c^2 \tag{A.1}$$

$$= n_{\mathrm{e,cr}} \int_0^\infty dp\, f_{\mathrm{e}}(p)\, (\sqrt{1+p^2} - 1)\, m_{\mathrm{e}} c^2 \tag{A.2}$$

$$= \frac{n_{\mathrm{e,cr}} m_{\mathrm{e}} c^2}{[p^{1-\alpha}]_{p_2}^{p_1}} \left[\frac{1}{2} \mathrm{B}_{\frac{1}{1+p^2}} \left(\frac{\alpha-2}{2}, \frac{3-\alpha}{2} \right) + p^{1-\alpha} \left(\sqrt{1+p^2} - 1 \right) \right]_{p_2}^{p_1} \tag{A.3}$$

$$\approx \frac{\alpha - 1}{\alpha - 2} \frac{[p^{2-\alpha}]_{p_2}^{p_1}}{[p^{1-\alpha}]_{p_2}^{p_1}} n_{\mathrm{e,cr}} m_{\mathrm{e}} c^2 \tag{A.4}$$

$$\approx \frac{\alpha - 1}{\alpha - 2} n_{\mathrm{e,cr}} m_{\mathrm{e}} c^2 p_1 \tag{A.5}$$

Here, we have used the short-hand notation defined in Eq. (29). The first approximation assumes the particles to be ultra-relativistic ($1 \ll p_1 < p_2$), and the second that the distribution is dominated by the lower end ($p_1 \ll p_2$ and $\alpha > 2$). For an ultra-relativistic population of electrons (and similar for protons) the pressure is $P_{\mathrm{e}} = \frac{1}{3}\varepsilon_{\mathrm{e}}$, but this is not correct for a transrelativistic population. There

$$P_{\rm e} = n_{\rm e,cr} \int_0^\infty dp\, f_{\rm e}(p)\, \frac{1}{3}\, p\, v(p)\, m_{\rm e}\, c \quad \text{(A.6)}$$

$$= \frac{n_{\rm e,cr}\, m_{\rm e}\, c^2\, (\alpha-1)}{6\, [p^{1-\alpha}]_{p_2}^{p_1}} \left[{\rm B}_{\frac{1}{1+p^2}} \left(\frac{\alpha-2}{2}, \frac{3-\alpha}{2} \right) \right]_{p_2}^{p_1} \quad \text{(A.7)}$$

$$\approx \frac{1}{3}\, \frac{\alpha-1}{\alpha-2}\, \frac{[p^{2-\alpha}]_{p_2}^{p_1}}{[p^{1-\alpha}]_{p_2}^{p_1}}\, n_{\rm e,cr}\, m_{\rm e}\, c^2 \approx \frac{1}{3}\, \varepsilon_{\rm e} \quad \text{(A.8)}$$

The ultra-relativistic approximation was again applied, assuming $1 \ll p_1 < p_2$. If this is not justified, correct results can easily be obtained from Eqs. (A.3) and (A.7).

Appendix B: Detectability of the cluster-rSZ-effect with multifrequency experiments

In order to demonstrate that the predicted non-thermal CMB distortions in the clusters like the Coma cluster (Sect. 5.2) are detectable with multifrequency experiments we estimate the expected sensitivity of the Planck satelitte. The spectral distortions at the location of the observed cluster are produced by temperature fluctuations of the CMB on the scale of the cluster ($\delta T/T \approx 10^{-6}...10^{-5}$), the thSZ and kSZ effect of the ICM gas, and the rSZ effect of the non-thermal electron distribution. The resulting distortion are therefore

$$\delta i(x) = \sum_{j=1}^{3} \tau_j\, f_j(x), \quad \text{(B.1)}$$

with

$$\tau_1 = \tau_{\rm th}, \;\; f_1(x) = j_{\rm th}(x) - i(x),$$
$$\tau_2 = \tau_{\rm rel}, \;\; f_2(x) = j_{\rm rel}(x) - i(x),$$
$$\tau_3 = \delta T/T + \bar{\beta}_{\rm gas}, \;\; f_3(x) = h(x)\,.$$

Here, $j_{\rm rel}(x)$ are the spectral distorions produced by the electrons in the non-thermal tail with optical thickness $\tau_{\rm rel}$ and spectrum given by $f_{\rm e,th\&cr}(p;\beta_{\rm th},\alpha,p_1,p_2) - f_{\rm e,th}(p;\beta_{\rm th})$ (with proper normalization).

The observing frequencies and sensitivities of the channels (k) of the Planck satelitte are taken from Puget (1998) and given in Table 2. We assume the beams to be Gaussian, and therefore to have the areas $A_k = 1.13\,{\rm FWHM}_k^2$. The core region of the Coma cluster is $A_{\rm Coma} \approx \pi\, r_{\rm core}^2 \approx 300\,{\rm arcmin}^2$. Thus, for each frequency $N_k = A_{\rm Coma}/A_k$ independent beams probe the CMB. Using a χ^2 analysis allows to dissentangle the different spectral distortions if sufficient multichannel sensitivity is given. The accuracy in the determination of τ_j is given by $\Delta\tau_j = \sqrt{C_{jj}}$, where $C = A^{-1}$ and

$$A_{jl} = \sum_k N_k\, \frac{f_j(x_k)\, f_l(x_k)}{(\Delta i(x_k))^2} \quad \text{(B.2)}$$

(Press et al. 1992). Assuming $\tau_{\rm th} = 5.95 \cdot 10^{-3}$ and $\tau_{\rm rel}$ and $j_{\rm rel}$ according to the models 1,2, and 3 (see Sect. 5.2) we find that $\tau_{\rm rel}/\Delta\tau_{\rm rel} = 0.61, 1.15, 0.96$ correspondingly. This demonstrates that the Planck mission is expected to give a marginal (1-sigma) detection of such a supra-thermal electron population in the Coma cluster. Since some other clusters are also expected to contain supra-thermal electrons – e.g. Abell 2256 revealed very recently a similar HEX excess (Fusco-Femiano et al. 2000) – a combined signal from several (HEX excess selected, or merger and post-merger) clusters might be detectable with statistical significance by Planck. This demonstrates the ability of future sensitive multichannel CMB telescopes – e.g. dedicated baloon experiments – to detect supra-thermal electron populations in clusters of galaxies.

References

Abramowitz M., Stegun I.A., 1965, Handbook of Mathematical Functions. Dover, New York

Begelman M.C., Cioffi D.F., 1989, ApJ 345, L21

Bersanelli M., Bouchet F.R., Efstathiou G., et al., 1996, 'COBRAS/SAMBA, Report on Phase A Study', ESA Report D/SCI(96)3; see also http://astro.estec.esa.nl/Planck

Birkinshaw M., 1999, Phys. Rep. 310, 97

Blasi P., 2000, ApJ 532, L9

Blumenthal G.R., Gould R.J., 1970, Rev. Mod. Phys. 42, 237

Böhringer H., Nulsen P.E.J., Braun R., Fabian A.C., 1995, MNRAS 274, L67

Bowyer S., Berghöfer T.W., 1998, ApJ 506, 502

Briel U.G., Henry J.P., Böhringer H., 1992, A&A 259, L31

Carilli C.L., Barthel P.D., 1996, A&AR 7, 1

Carilli C.L., Harris D.E., 1996, In: Carilli C.L., Harris D.E. (eds.) Proceedings of the Greenbank workshop, held in Greenbank, West Virginia, May 1-4, 1995, Cambridge University Press, Cambridge

Chandrasekhar S., 1950, Radiative Transfer. Oxford, Clarendon Press, p. 17

Chokshi A., Turner E.L., 1992, MNRAS 259, 421

Clarke D.A., Harris D.E., Carilli C.L. 1997, MNRAS284, 981

Crusius-Waetzel A.R., Biermann P.L., Schlickeiser R., Lerche I., 1990, ApJ 360, 417

Daly R.A., 1999, In: Biretta, et al. (eds.) Life Cycles of Radio Galaxies. New Astronomy Reviews, in press

Dogiel V.A., 1999, In: Böhringer H., Feretti L., Schuecker P. (eds.) Ringberg Workshop, Diffuse Thermal and Relativistic Plasma in Galaxy Clusters. MPE Report No. 271, p. 259

Dunlop J.S., Peacock J.A., 1990, MNRAS 247, 19

Enßlin T.A., 1999, In: Böhringer H., Feretti L., Schuecker P. (eds.) Ringberg Workshop, Diffuse Thermal and Relativistic Plasma in Galaxy Clusters. MPE Report No. 271, p. 275

Enßlin T.A., Biermann P.L., 1998, A&A 330, 90

Enßlin T.A., Biermann P.L., Kronberg P.P., Wu X.-P., 1997, ApJ 477, 560

Enßlin T.A., Biermann P.L., Klein U., Kohle S., 1998a, A&A 332, 39

Enßlin T.A., Wang Y., Nath B.B., Biermann P.L., 1998b, A&A 333, L47

Enßlin T.A., Lieu R., Biermann P.L., 1999, A&A 344, 409

Faber S.M., Tremaine S., Ajahr E.A., et al., 1997, AJ 114, 1771

Fabian A.C., 1999, Bologna Conference, astro-ph/0001178

Fabian A.C., Iwasawa K., 1999, MNRAS 303, L34

Falle S.A.E.G, 1991, MNRAS 250, 581

Fargion D., Salis A., 1998, Phys. Usp. 41, 823; 1998, Usp.Fiz.Nauk 168, 909

Fargion D., Konopolich R.V., Salis A., 1996, preprint, astro-ph/9606126

Feretti L., Giovannini G., 1996, In: Ekers R., Fanti C., Padrielli L. (eds.) IAU Symp. 175, Extragalactic Radio Sources. Kluwer Academic Publisher, p. 333
Feretti L., Perola G.C., Fanti R., 1992, A&A 265, 9
Feretti L., Dallacasa D., Giovannini G., Tagliani A., 1995, A&A 302, 680
Feretti L., Dallacasa D., Govoni F., et al., 1999, A&A 344, 472
Fixsen D.J., Cheng E.S., Gales J.M., et al. 1996, ApJ 473, 576
Fusco-Femiano R., Dal Fiume D., Feretti L., et al., 1998, Proceedings of 32nd COSPAR Scientific Assembly, Nagoya, Japan, in press, astro-ph/9808012
Fusco-Femiano R., Dal Fiume D., Feretti L., et al., 1999, ApJ 513, L21
Fusco-Femiano R., Dal Fiume D., De Grandi S., et al., 2000, ApJ 534, L7
Greisen K., 1966, Phys. Rev. Lett. 16, 748
Hwang C.-Y., 1997, Sci 278, 1917
Jaffe W.J., 1992, In: Fabian A.C. (ed.) Clusters and Superclusters of Galaxies. Kluwer Academic Publisher, Dordrecht, p. 109
Kaiser C.R., Alexander P., 1997, MNRAS 286, 215
Kaiser C.R., Alexander P., 1999, MNRAS 305, 707
Kaiser C.R., Dennett-Thorpe J., Alexander P., 1997, MNRAS 292, 723
Kaiser C.R., Schoemakers A.P., Röttgering H.J.A., 2000, MNRAS 315, 381
Kardashev N.S., 1962, SvA AJ 6, 317
Kim K.-T., Kronberg P.P., Tribble P.C. 1991, ApJ 379, 80
Lieu R., Mittaz J.P.D., Bowyer S., et al., 1996, Sci 274, 1335
Longair M.S., Sunyaev R.A., 1971, The Electromagnetic Radiation in the Universe. Usp. Fiz. Nauk. 105, No. 1, 41; 1972, Soviet Phisics (Uspekhi) 14, No. 5, 569
McKinnon M.M., Owen F.N., Eilek J.A., 1991, AJ 101, 2026
McNamara B.R., Wise M., Nulsen P.E.J., et al., 2000, ApJ 534, L135
Molnar S.M., Birkinshaw M., 1999, ApJ523, 78
Press W.H., Teukolsky S.A., Vetterling W.T., Flannery B.P., 1992, Numerical Recipes in C. 2nd Edition, Cambridge University Press
Puget J.-L., 1998, Planck/HFI proposal to ESA, see also http://astro.estec.esa.nl/Planck/technical/payl/node7.html
Rawlings S., Saunders R., 1991, Nat 349, 138
Rephaeli Y., 1979, ApJ 227, 364
Rephaeli Y., 1995a, ApJ 445, 33
Rephaeli Y., 1995b, ARA&A 33, 541
Sarazin C.L., Lieu R., 1998, ApJ 494, 177
Sarazin C.L., Kempner J.C., 2000, ApJ 533, 73
Sazonov S.Y., Sunyaev R.A., 2000, A&A354, L53
Soltan A., 1982, MNRAS 200, 115
Sunyaev, R.A., Zeldovich Y.B., 1980, ARA&A 18, 537
Wright E.L., 1979, ApJ 232, 348
Yamada M., Sugiyama N., Silk J., 1999, ApJ 522, 66
Zatsepin G.T., Kuzmin V.A., 1966, Pis'ma Zh. Eksp. Teor. Fiz. 4, 144; 1996, JETP. Lett. 4, 78
Zeldovich Ya.B., Illarionov A.F., Sunyaev R.A., 1972, Zh. Eksp. Theor. Fiz. 62, No. 4, 1217; 1973, Soviet Physics (JETP) 35, No. 4, 643